Location of Subunit d in the Peripheral Stalk of the ATP Synthase from *Saccharomyces cerevisiae*[†]

Stephanie A. Bueler[‡] and John L. Rubinstein*[,‡,§]

Molecular Structure and Function Program, The Hospital for Sick Children Research Institute, and Department of Biochemistry, University of Toronto, Toronto, Ontario, Canada

Received September 2, 2008; Revised Manuscript Received September 23, 2008

ABSTRACT: ATP synthase from *Saccharomyces cerevisiae* is an ~600 kDa membrane protein complex. The enzyme couples the proton motive force across the mitochondrial inner membrane to the synthesis of ATP from ADP and inorganic phosphate. The peripheral stalk subcomplex acts as a stator, preventing the rotation of the soluble F_1 region relative to the membrane-bound F_O region during ATP synthesis. Component subunits of the peripheral stalk are Atp5p (OSCP), Atp4p (subunit b), Atp7p (subunit d), and Atp14p (subunit h). X-ray crystallography has defined the structure of a large fragment of the bovine peripheral stalk, including 75% of subunit d (residues 3−123). Docking the peripheral stalk structure into a cryo-EM map of intact yeast ATP synthase showed that residue 123 of subunit d lies close to the bottom edge of F_1. The 37 missing C-terminal residues are predicted to either fold back toward the apex of F_1 or extend toward the membrane. To locate the C terminus of subunit d within the peripheral stalk of ATP synthase from *S. cerevisiae*, a biotinylation signal was fused to the protein. The biotin acceptor domain became biotinylated in vivo and was subsequently labeled with avidin in vitro. Electron microscopy of the avidin-labeled complex showed the label tethered close to the membrane surface. We propose that the C-terminal region of subunit d spans the gap from F_1 to F_O, reinforcing this section of the peripheral stalk.

The mitochondrial ATP synthase is a membrane-bound protein complex that catalyzes the formation of ATP from ADP and inorganic phosphate. The enzyme is composed of a membrane-embedded F_O region and a globular F_1 region that protrudes into the mitochondrial matrix and is connected to F_O by a central stalk and a peripheral stalk (*1*). Low-resolution models of the intact complexes from bovine heart and *Saccharomyces cerevisiae* mitochondria are available from electron cryomicroscopy of single particles (cryo-EM)[1] (*2, 3*), and high-resolution models have been determined by X-ray crystallography of bovine, chloroplast, yeast, and *Bacillus* sp. TA2.A1 F_1-ATPase (*4*−*7*).

In yeast mitochondria, the F_O region of ATP synthase utilizes the proton motive force across the mitochondrial inner membrane to drive ATP synthesis in F_1. As protons pass from the intermembrane space to the mitochondrial matrix via a pore between subunit a and a ring of 10 c subunits, a force is generated that leads to the rotation of the central rotor complex (subunits $\gamma\delta\varepsilon$-c_{10}) (*8*−*10*). Rotation of the central stalk causes conformational changes in the catalytic nucleotide binding sites of the β subunits, which sequentially pass through the series of states necessary for ATP synthesis (*8, 11*).

The peripheral stalk resists the tendency of the $\alpha_3\beta_3$ hexamer to rotate along with the central stalk, and disruption of the peripheral stalk uncouples proton translocation from ATP synthesis (*12*). The bacterial peripheral stalk consists of the δ- and b-subunits (*13*), the latter of which must form a dimer to bind to F_1 (*14*). The eukaryotic complex is composed of single copies of the oligomycin sensitivity conferral protein (OSCP), subunit b, subunit d, and subunit h (F_6 in the bovine enzyme) (*15, 16*). OSCP, which is homologous to the bacterial δ-subunit, binds to the end of F_1 distal from F_O (*17*−*19*), and its C terminus extends ~90 Å along the surface of F_1 to a point where it interacts with subunit b (*15, 16, 20*). Subunit b continues along the same trajectory into the membrane where it contains two transmembrane helices (*21*). Most of subunit h or F_6 lies near the F_1 end of the peripheral stalk and interacts with subunits b and d (*22*), while its C terminus extends close to the membrane in the yeast enzyme (*23*).

An atomic model of a portion of the bovine peripheral stalk subcomplex, containing subunits b (residues 79−183 of 214), d (residues 3−123 of 160), and F_6 (residues 5−70 of 76), was obtained by X-ray crystallography (*22*), and a model of the N-terminal domain of bovine OSCP was determined by solution NMR spectroscopy (*18*). Sequence alignments for the bovine and yeast peripheral stalk subunits (Figure 1) exhibit remarkable conservation, with the exception of subunit h which can nonetheless functionally substitute for F_6 (*24*). Mapping of known α-helices from the X-ray and NMR models onto the sequences and comparison

[†] J.L.R. was supported by a New Investigator Award from the CIHR, and this work was funded by Operating Grant MOP 81294 from the CIHR.

* To whom correspondence should be addressed: 555 University Ave., Toronto, Ontario, Canada M5G 1X8. Telephone: (416) 813-7255. Fax: (416) 813-5022. E-mail: john.rubinstein@utoronto.ca.

[‡] The Hospital for Sick Children Research Institute.

[§] University of Toronto.

[1] Abbreviations: cryo-EM, electron cryomicroscopy; EM, electron microscopy; OSCP, oligomycin sensitivity conferral protein.

10.1021/bi801665x CCC: $40.75
Published on Web 10/21/2008

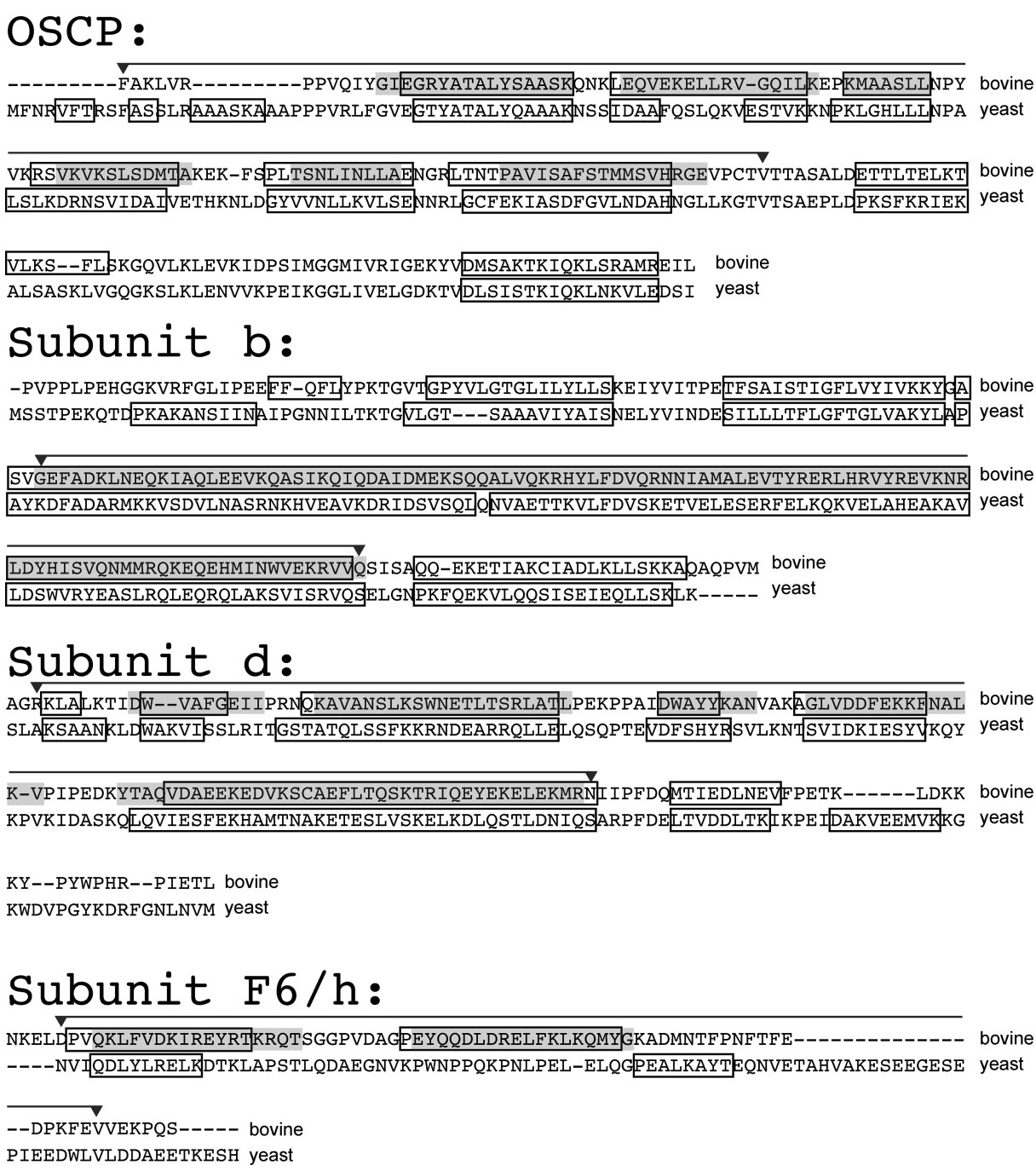

FIGURE 1: Sequence alignment and structure prediction for bovine and yeast peripheral stalk subunits. Sequence alignment was performed with MUSCLE 3.6 (*31*) and secondary structure prediction with JPRED (*32*). Experimental information about the secondary structure of bovine peripheral stalk subunits b, d, and F_6 is from crystal structure 2CLY (*22*) containing subunits b (residues 79−183 of 214), d (residues 3−123 of 160), and F_6 (residues 5−70 of 76). Experimental information about the secondary structure of the bovine N-terminal domain of OSCP (residues 1−120 of 190) is from solution NMR structure 2BO5 (*18*). Experimentally observed secondary structure is shaded in gray, and a line above the sequence indicates the residues seen in the crystal structure. Predicted secondary structure from JPRED is drawn with a box around it.

with results of secondary structure prediction algorithms show that secondary structure motifs can be effectively predicted in these subunits. The crystal structure of the peripheral stalk fragment can be docked into the cryo-EM map of the yeast ATP synthase (Figure 2) (*3*). Although the truncated C terminus of subunit d (residue 123) is oriented toward the membrane, it was proposed that the 37 missing residues make another turn to terminate facing the top of F_1. Therefore, an outstanding question in understanding the topology of the eukaryotic peripheral stalk is the location of the C-terminal region of subunit d. Figure 2 shows that residue 123 of subunit d lies approximately at the same height as the bottom of the α- and *β*-subunits. The 37 remaining residues of subunit d, if fully α-helical, could be displaced by as much as 56 Å from this location. If subunit d adopts a "paper clip" conformation in the intact complex, then the C terminus of subunit d (residue 160) would be predicted to lie as indicated by the top arrow in Figure 2, while the lower arrow indicates the probable location of the C terminus of subunit d if it does not bend near residue 123.

To determine the location of the C-terminal end of subunit d within the peripheral stalk of the yeast ATP synthase, a

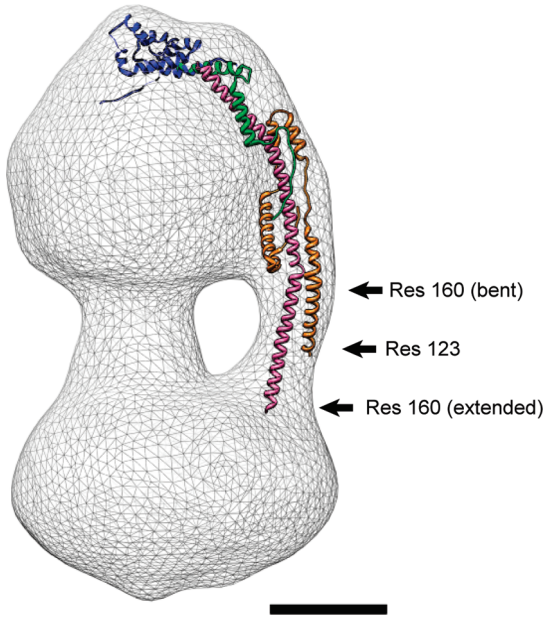

FIGURE 2: Docking of the peripheral stalk subunit models into the yeast ATP synthase map. The three-dimensional map of yeast ATP synthase at 24 Å resolution is shown as a gray mesh (*3*). The crystal structure of the bovine peripheral stalk fragment (*22*) was docked into the EM map and is shown with subunit b colored pink (residues 79−183 of 214), subunit d orange (residues 3−123 of 160), and subunit F_6 green (residues 5−70 of 76). The N-terminal domain of bovine OSCP (*18*) is colored in blue. Arrows indicate the observed position of the truncated residue 123 of subunit d and the predicted positions of the true C terminus of the subunit (residue 160) if the C-terminal 25% of residues from subunit d formed an α-helix that bent toward F_1 or continued to the membrane surface. The scale bar represents 50 Å.

labeling system was employed incorporating a biotinylation signal sequence from the transcarboxylase enzyme of *Propioniobacterium shermanii*. The transcarboxylase sequence forms a compact folded domain that has been shown to be recognized and biotinylated in vivo by the endogenous biotin ligase of *S. cerevisiae* (*25*). Using the biotinylation signal sequence to localize subunits by single-particle electron microscopy has three requirements. (1) The sequence must be successfully expressed and not cleaved from the fusion protein. (2) In vivo biotinylation of the sequence must occur with a large fraction of protein particles. (3) In vitro labeling of the biotin with avidin must occur stoichiometrically or nearly stoichiometrically (*20, 23*). Successful incorporation of the signal sequence can be monitored by SDS−PAGE, where the modified protein will shift upward with the addition of ~8 kDa of mass from the signal. Biotinylation of the protein can be detected by Western blotting, and if the Western blot signal disappears entirely after the complex is incubated with avidin, this experiment indicates that all available biotin has been labeled with avidin. However, Western blotting does not easily reveal the fraction of the signal sequences that have been biotinylated. Fortunately, once avidin is bound to the biotinylated protein, the complex does not become dissociated under SDS−PAGE conditions (unless heated) and the glycosylated avidin is retained in the stacking gel. Therefore, stoichiometric biotinylation and avidin labeling can be detected by the complete disappearance of the subunit band from a SDS−PAGE gel after incubation of the complex with avidin.

We determined that a linker sequence between the C terminus of subunit d and the biotinylation signal is necessary for stoichiometric biotinylation in vivo. Labeling the biotinylated subunit d in vitro allowed us to localize the C terminus of subunit d and showed that the sequence not described by the crystal structure extends toward the membrane region of the complex. We use the information from these experiments to propose a model of the structure of the peripheral stalk complex in the ATP synthase from *S. cerevisiae*. Specifically, we propose that the C-terminal region of subunit d contributes to the observed density of the F_1 to F_O connection seen in the cryo-EM model and thereby strengthens this link.

EXPERIMENTAL PROCEDURES

Modification of the ATP7 Gene and Purification of the Modified ATP Synthase. USY006, a *S. cerevisiae* strain with the sequence encoding a hexahistidine tag fused to the N terminus of the *ATP2* gene (β-subunit), was a gift from D. Mueller (Rosalind Franklin University, North Chicago, IL). The strain was genetically manipulated further to encode a biotinylation signal sequence C-terminal to subunit d. PCR with the Expand High Fidelity PCR System (Roche, Laval, QC) was used to generate a DNA fragment for homologous recombination. The fragment consisted of a 5′ region homologous to the 3′ end of the *ATP7* gene and 3′ region homologous to the genomic DNA downstream of the *ATP7* gene. The central sequence of the DNA fragment encoded a biotinylation signal sequence (either with or without a linker sequence) followed by the *URA3* auxotrophic marker from *Candida albicans*. The template DNA for the PCR, a gift from M. Kampmann (Rockefeller University, New York, NY), was plasmid pMK159, which encodes an 8 kDa biotinylation signal sequence from *P. shermanii* followed by the *C. albicans URA3* marker. The forward primer was 5′-AAT GGG ACG TAC CTG GTT ACA AGG ACA GAT TCG GCA ATT TGA ATG TGA TGG CCG GTA AGG CCG GAG AGG G-3′ (without linker) or 5′-AAT GGG ACG TAC CTG GTT ACA AGG ACA GAT TCG GCA ATT TGA ATG TGA TGG CAC TAA ATG TAG CAC TAG CCG GTA AGG CCG GAG AGG G-3′ (to include an 18-nucleotide linker sequence) and corresponded to the 50 bases upstream of the *ATP7* gene stop codon and the first 20 bases of the biotinylation signal sequence. The reverse primer in both cases, 5′-TGT GAA AAA AAT AAT AGA ATA TGG TGC GTA ATA TAT AGA GGT AAA GGG TAA TAT CAT CGA TGA ATT CGA GCT CG-3′, consisted of the reverse and complement of the 50 bases downstream of (and excluding) the stop codon of the *ATP7* gene and 24 bases of the reverse and complement of the pMK159 plasmid DNA downstream of the *URA3* marker gene. The DNA fragment was incorporated into the USY006 genome by homologous recombination, and yeast colonies containing the modified gene were selected by growth on SD medium lacking uracil (*26*). Successful integration of the sequences was verified by PCR using the forward primer 5′-AGA GAT GGT CAA GAA GGG TAA-3′ and the reverse primer 5′-GAT CTT GAT GAG ACC CTG AC-3′.

ATP synthase with a biotinylation signal at the C terminus of subunit d was isolated and labeled with avidin as described previously (*23*) except using a BioFlo benchtop fermentor

(New Brunswick Scientific, Edison, NJ) to grow the yeast culture. Recombinant BirA biotin ligase was obtained from Avidity LLC (Denver, CO) and was used according to the manufacturer's instructions.

SDS−PAGE and Western Blotting. ATP synthase purified from USY006 and the Atp7-bio strains were run on Novex 4 to 12% Bis-Tris NuPAGE gels (Invitrogen Corp., Carlsbad, CA) that were either stained with Coomassie or transferred to nitrocellulose membranes and incubated with ExtrAvidin−peroxidase conjugate (Sigma-Aldrich Canada Ltd., Oakville, ON) diluted 1:10000. Peroxidase activity was detected by enhanced chemiluminescence (Pierce Biotechnology, Rockford, IL).

Electron Microscopy and Image Analysis. Negative stain EM specimen preparation was conducted as described previously (*23, 27*). Electron microscopy was performed with a FEI Co. (Eindhoven, The Netherlands) Tecnai F20 electron microscope equipped with a field emission gun and operating at 200 kV. Images were recorded at a magnification of 50000× on SO-163 film (Kodak Canada, Toronto, ON), developed for 12 min in full-strength Kodak D19 developer and digitized with an Intergraph PhotoScan (Huntsville, AL) densitometer at a step size of 7 μm. Adjacent pixels were averaged 3 × 3 to give a final sampling of 4.2 Å/pixel. Particles were selected with Ximdisp (*28*) and filtered with an Imagic-like filter (*29*). Alignment and classification of images were conducted with SPIDER (*30*).

Sequence Comparison and Secondary Structure Prediction. Bovine and yeast peripheral stalk subunit sequences were aligned using MUSCLE (*31*), and secondary structure was predicted with JPRED (*32*) specifically excluding the known ATP synthase subunit structures from the data used by the algorithm.

RESULTS

Genetic Manipulation of S. cerevisiae. S. cerevisiae strain USY006 contains N-terminal hexahistidine-tagged β-subunits. This strain was further modified to include signal sequences fused to the C terminus of Atp7p, ATP synthase subunit d. The fusion proteins were created by modifying the yeast genomic DNA via homologous recombination. Modification of subunit d did not appear to affect the growth or function of ATP synthase as the strain was able to grow on the nonfermentable medium YPG and the rate of growth was not reduced.

Biochemical Characterization of the Atp7 Fusion Strains. ATP synthase was purified by metal affinity chromatography followed by gel filtration chromatography, and the complex was analyzed by SDS−PAGE and Western blotting. Initial attempts (results not shown) to fuse the folded 75-residue transcarboxylase domain to subunit d produced a complex with the d subunit mass increased from 20 to 28 kDa. Western blotting indicated that the fusion protein had been covalently modified with biotin, and the complete disappearance of the Western blot signal after incubation with avidin indicated stoichiometric labeling of the available biotin with avidin. However, mixing the complex with avidin did not lead to the complete disappearance of the subunit d band from a Coomassie-stained SDS−PAGE gel, suggesting incomplete biotinylation of the subunit by the endogenous biotin ligase in vivo. Attempts to use recombinant BirA biotin ligase in vitro to increase the proportion of subunit d fusion protein modified with biotin did not lead to an increase in the level of biotinylated enzyme, nor did use of a 15-residue biotin acceptor sequence, GLNDIFEAQKIEWHE (www.avidity.com). A logical alternative to the biotin−avidin labeling approach, introduction of a maltose binding protein label on the subunit of interest, resulted in a strain of yeast that was not able to survive on nonfermentable medium.

Subsequently, a strain of yeast was constructed with a six-amino acid linker sequence (ALNVAL) separating the biotinylation signal domain from the C terminus of subunit d. Once again, SDS−PAGE showed an increase in mass of approximately 8 kDa for the subunit d fusion protein relative to the unmodified subunit d (Figure 3A, first and second lanes). Western blotting confirmed biotinylation of subunit d (Figure 3B, first and second lanes) that could be completely labeled with avidin in vitro (Figure 3B, third lane). This time, however, incubating the complex with avidin led to the complete disappearance of the subunit d band from the Coomassie-stained SDS−PAGE gel (Figure 3A, third lane). Taken together, these results indicated that the biotinylation signal sequence fused to subunit d via a six-residue linker sequence was recognized and stoichiometrically biotinylated in vivo by the endogenous yeast biotin ligase enzyme and stoichiometrically labeled with avidin in vitro.

Electron Microscopy. After being labeled with avidin, ATP synthase with the subunit d fusion protein was stained and imaged by electron microscopy. The majority of the images of individual complexes had the bilobed structure seen previously for yeast ATP synthase (*20*). In most particles, an additional density, corresponding to the avidin label, was observed to the right of F_O when the complex was represented with F_1 above F_O (Figure 3C).

A data set of 1501 images of labeled complex in which F_1, F_O, and avidin could be clearly seen was selected interactively. Images were aligned by reference-free methods and separated into five classes by multivariate data analysis (*30*). Figure 4A−E shows the five class averages generated. Four of the five class averages show the avidin label to the right of the complex, while the fifth (Figure 4E) shows the avidin label to the left. Figure 4F shows the average of all of the aligned particles. Figure 4G shows an overlay of the overall sum image with a view of the three-dimensional model of yeast ATP synthase and the relative locations of the four avidin labels to the right of the complex. There was little variability in the position of the avidin label, suggesting that the linker region lacks flexibility by being constrained. A narrow arc centered on the peripheral stalk and describing the positions of all of the labels indicated that the position of the C terminus of subunit d is immediately above the membrane region of the complex. This observation rules out a paper clip conformation for subunit d in yeast and instead supports an extending helix for the C-terminal region of the protein with the 37 C-terminal residues of subunit d spanning the distance from the bottom edge of F_1 to the membrane surface of F_O.

DISCUSSION

The location of the C terminus of subunit d described above is similar to the location of the C terminus of subunit

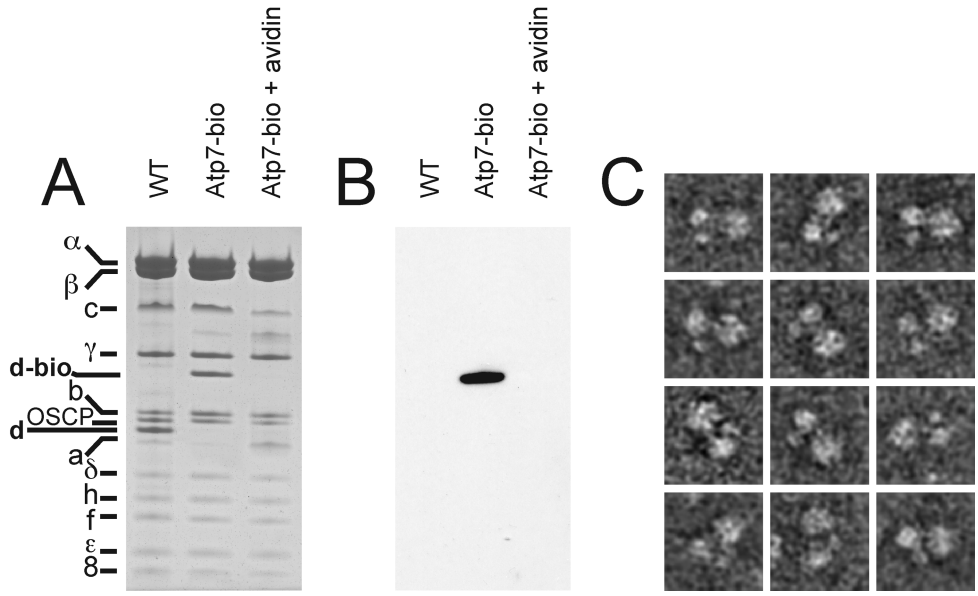

FIGURE 3: Introduction of a biotinylation signal sequence at the C terminus of subunit d. (A) Analysis by SDS−PAGE. A shift in mass of wild-type subunit d (WT lane) can be seen when the subunit is fused to a biotinylation signal sequence (Atp7-bio lane). Upon avidin labeling, the subunit d-bio band disappeared (Atp7-bio + avidin lane), indicating stoichiometric biotinylation and stoichiometric labeling with avidin. (B) Western blotting analysis with the ExtrAvidin−HRP conjugate. A band in the Atp7-bio lane confirmed the presence of biotin. Upon avidin labeling, the subunit band disappeared entirely, indicating that all available biotin had been labeled with avidin (Atp7-bio + avidin lane). (C) Some example images of avidin-labeled ATP synthase particles embedded in stain.

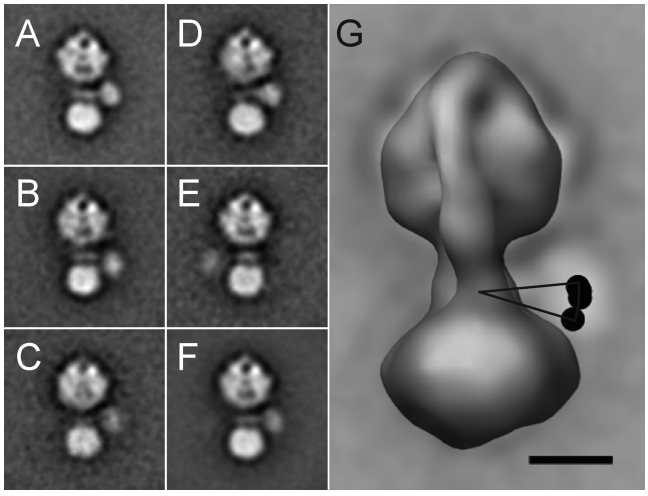

FIGURE 4: Image analysis of avidin-labeled Atp7-bio complex. (A−E) Five class average images generated by multivariate data analysis. (F) Average of all of the aligned particle images. (G) Overall average of the particle images shown in part F overlaid with a surface-rendered view of the three-dimensional map of yeast ATP synthase, oriented so that the peripheral stalk and central stalk overlap in projection [as seen before for ATP synthase bound to continuous carbon supports (*2, 20, 23*)]. The positions of the four avidin labels that lie to the right of the complex were plotted alongside the overlay, and an arc was drawn to indicate the most likely tethering point for the avidin label. This arc indicates that the C terminus of subunit d is located immediately above the membrane surface in the yeast ATP synthase. The scale bar in panel G represents 100 Å.

h as determined by similar experiments (*23*). However, compared with labeled subunit d, the avidin-labeled subunit h construct had no linker sequence between the biotinylation signal and the subunit yet exhibited a strikingly greater degree of flexibility for the avidin label. The more constrained motion of the label when attached to subunit d may suggest that the C terminus of this subunit is somewhat inaccessible, possibly due to being located on the central stalk-facing surface of the peripheral stalk. The fact that most class averages from the labeled h subunit showed the avidin to the left of the complex (F_1 above F_O) compared with the avidin lying to the right of the complex for the labeled d subunit could also indicate the side from which the peripheral stalk of the C terminus of each subunit is most accessible.

Cryo-EM models of the yeast and bovine ATP synthase complexes revealed noticeable differences between the peripheral stalks of the two enzymes (*2, 3*). The peripheral stalk of the bovine enzyme has a constriction immediately above the membrane, while the yeast complex has a uniform thickness as it joins F_1 to F_O. This physical connection between F_1 and F_O is believed to be the most important role of the peripheral stalk. The source of the differences in the cryo-EM model is almost certainly differences in the subunits that make up the peripheral stalk. Here, we have shown that the C-terminal region of yeast subunit d contributes to the portion of the peripheral stalk that joins F_1 to F_O. Therefore, the difference in the subunit d sequence in the bovine and yeast peripheral stalks would be seen in this region and is the likely cause of the different appearance of the bovine and yeast peripheral stalks. It has been demonstrated that subunit d interacts with subunits b, OSCP, and F_6 (*16*) and that during assembly subunit b binds the complex first, followed by OSCP and then subunit d (*33*). The requirement for subunit d may arise from its ability to stabilize the interaction between the other peripheral stalk subunits, particularly OSCP and b, which form a continuous link from the apex of F_1 to the membrane.

Information from structures determined for the bovine peripheral stalk subunits can be combined with labeling experiments in yeast to give a working model for the structure of the yeast peripheral stalk. The resulting model is shown in Figure 5. Residues 1−120 of OSCP form an N-terminal domain consisting of six α-helices (*18*). Yeast OSCP contains 22 more residues than bovine OSCP, 18 of

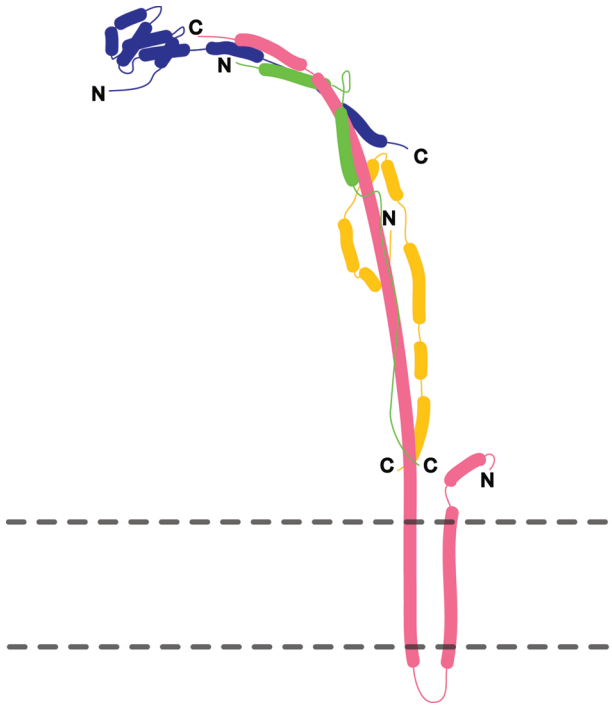

FIGURE 5: Proposed model of the yeast peripheral stalk subcomplex. In addition to the EM experiments, the model incorporates information from X-ray crystallography and solution NMR spectroscopy of the bovine peripheral stalk subunits and secondary structure prediction for the yeast subunits. OSCP (blue) forms an N-terminal domain that binds the apex of F_1 distal from F_O. The C-terminal region forms two predicted α-helices and continues along the surface of F_1 for approximately 90 Å. The N-terminal end of subunit b (pink) forms two transmembrane helices. Subunit b then continues up toward F_1 in a long, continuous helix. The C-terminal end of subunit b contains a predicted helix near the N-terminal domain of OSCP. Subunit h (green) forms two helices that wrap around the C-terminal end of the long subunit b α-helix. A long C-terminal extension of subunit h continues down the peripheral stalk until it is in the proximity of the membrane of the complex. Subunit d (orange) forms a five-helix structure with its N-terminal region. The C-terminal region of subunit d continues toward the membrane where it contains two short predicted helices and terminates near the C terminus of subunit h. The membrane is depicted as a broken gray line.

which are inserted near the N terminus in a region that is unstructured in bovine OSCP. Therefore, the N-terminal domain of OSCP in yeast is expected to end at approximately residue 138. The remaining sequence, from residue 139 to 212, is predicted to contain two α-helices and extend approximately 90 Å along the surface of F_1 (*20*). The crystal structure of the bovine peripheral stalk fragment shows a continuous α-helix for residues 79−183 of subunit b, which align with residues 78−182 of yeast subunit b. Residues 1−77 of yeast subunit b align with residues 1−78 of bovine subunit b. This region in both yeast and bovine subunit b is expected to continue toward the membrane to form the two transmembrane helices predicted for the N-terminal region of subunit b (*21*). The 27 remaining C-terminal residues of yeast subunit b are expected to lie near the OSCP subunit and are predicted to contain an additional α-helix. Of all of the peripheral stalk subunits, F_6/subunit h is the least conserved between the yeast and bovine enzymes (*24*). The bovine crystal structure contains two α-helices formed by residues 5−70 of subunit F_6 that correspond to residues 1−81 of yeast subunit h. The C terminus of the portion of F_6 in the crystal structure lies near the bottom edge of F_1. Yeast subunit h has 17 more residues than bovine subunit F_6 that take the C terminus of the yeast subunit close to the membrane (*23*). Subunit d has by far the most complicated structure of the peripheral stalk subunits. The yeast and bovine subunit d sequences align well with the 13 extra residues of the yeast subunit mostly found as short insertions near the C terminus of the protein. Residues 3−123 of the 160 residues in the bovine subunit form five α-helices in the crystal structure that resemble a paper clip missing its final turn that is wrapped around the other peripheral stalk proteins. Residue 123 in bovine subunit d aligns with residue 125 in the yeast protein, and from the data presented in this paper, residues 126−173 in the yeast protein extend further down the peripheral stalk, ending immediately above the membrane.

ACKNOWLEDGMENT

We thank Dr. David Mueller (Rosalind Franklin University) for providing the USY006 strain and Mr. Martin Kampmann (Rockefeller University) for the pMK159 plasmid containing the *P. shermanii* biotinylation signal with the *C. albicans* URA3 marker gene. We thank Drs. John Walker and David Mueller for critical reading of the manuscript.

REFERENCES

1. Walker, J. E. (1998) ATP synthesis by rotary catalysis (Nobel Lecture). *Angew. Chem., Int. Ed. 37*, 2309–2319.
2. Rubinstein, J. L., Walker, J. E., and Henderson, R. (2003) Structure of the mitochondrial ATP synthase by electron cryomicroscopy. *EMBO J. 22*, 6182–6192.
3. Lau, W. C. Y., Baker, L. A., and Rubinstein, J. L. (2008) Cryo-EM structure of the yeast ATP synthase. *J. Mol. Biol. 382*, 1256–1264.
4. Gibbons, C., Montgomery, M. G., Leslie, A. G., and Walker, J. E. (2000) The structure of the central stalk in bovine F_1-ATPase at 2.4 Å resolution. *Nat. Struct. Biol. 7*, 1055–1061.
5. Groth, G., and Pohl, E. (2001) The structure of the chloroplast F1-ATPase at 3.2 Å resolution. *J. Biol. Chem. 276*, 1345–1352.
6. Kabaleeswaran, V., Puri, N., Walker, J. E., Leslie, A. G., and Mueller, D. M. (2006) Novel features of the rotary catalytic mechanism revealed in the structure of yeast F1 ATPase. *EMBO J. 25*, 5433–5442.
7. Stocker, A., Keis, S., Vonck, J., Cook, G. M., and Dimroth, P. (2007) The Structural Basis for Unidirectional Rotation of Thermoalkaliphilic F_1-ATPase. *Structure 15*, 904–914.
8. Abrahams, J. P., Leslie, A. G., Lutter, R., and Walker, J. E. (1994) Structure at 2.8 Å resolution of F1-ATPase from bovine heart mitochondria. *Nature 370*, 621–628.
9. Sambongi, Y., Iko, Y., Tanabe, M., Omote, H., Iwamoto-Kihara, A., Ueda, I., Yanagida, T., Wada, Y., and Futai, M. (1999) Mechanical rotation of the c subunit oligomer in ATP synthase (F_0F_1): Direct observation. *Science 286*, 1722–1724.
10. Stock, D., Leslie, A. G., and Walker, J. E. (1999) Molecular architecture of the rotary motor in ATP synthase. *Science 286*, 1700–1705.
11. Boyer, P. D. (1997) The ATP synthase: A splendid molecular machine. *Annu. Rev. Biochem. 66*, 717–749.
12. Walker, J. E., and Dickson, V. K. (2006) The peripheral stalk of the mitochondrial ATP synthase. *Biochim. Biophys. Acta 1757*, 286–296.
13. Dunn, S. D., McLachlin, D. T., and Revington, M. (2000) The second stalk of *Escherichia coli* ATP synthase. *Biochim. Biophys. Acta 1458*, 356–363.
14. Sorgen, P. L., Bubb, M. R., McCormick, K. A., Edison, A. S., and Cain, B. D. (1998) Formation of the b subunit dimer is necessary for interaction with F1-ATPase. *Biochemistry 37*, 923–932.

15. Collinson, I. R., Skehel, J. M., Fearnley, I. M., Runswick, M. J., and Walker, J. E. (1996) The F1F0-ATPase complex from bovine heart mitochondria: The molar ratio of the subunits in the stalk region linking the F1 and F0 domains. *Biochemistry 35*, 12640–12646.
16. Collinson, I. R., van Raaij, M. J., Runswick, M. J., Fearnley, I. M., Skehel, J. M., Orriss, G. L., Miroux, B., and Walker, J. E. (1994) ATP synthase from bovine heart mitochondria. In vitro assembly of a stalk complex in the presence of F1-ATPase and in its absence. *J. Mol. Biol. 242*, 408–421.
17. Hundal, T., Norling, B., and Ernster, L. (1983) Lack of ability of trypsin-treated mitochondrial F1-ATPase to bind the oligomycin-sensitivity conferring protein (OSCP). *FEBS Lett. 162*, 5–10.
18. Carbajo, R. J., Kellas, F. A., Runswick, M. J., Montgomery, M. G., Walker, J. E., and Neuhaus, D. (2005) Structure of the F1-binding domain of the stator of bovine F1Fo-ATPase and how it binds an α-subunit. *J. Mol. Biol. 351*, 824–838.
19. Carbajo, R. J., Kellas, F. A., Yang, J. C., Runswick, M. J., Montgomery, M. G., Walker, J. E., and Neuhaus, D. (2007) How the N-terminal domain of the OSCP subunit of bovine F1Fo-ATP synthase interacts with the N-terminal region of an α subunit. *J. Mol. Biol. 368*, 310–318.
20. Rubinstein, J. L., and Walker, J. E. (2002) ATP synthase from *Saccharomyces cerevisiae*: Location of the OSCP subunit in the peripheral stalk region. *J. Mol. Biol. 321*, 613–619.
21. Walker, J. E., Runswick, M. J., and Poulter, L. (1987) ATP synthase from bovine mitochondria. The characterization and sequence analysis of two membrane-associated sub-units and of the corresponding cDNAs. *J. Mol. Biol. 197*, 89–100.
22. Dickson, V. K., Silvester, J. A., Fearnley, I. M., Leslie, A. G., and Walker, J. E. (2006) On the structure of the stator of the mitochondrial ATP synthase. *EMBO J. 25*, 2911–2918.
23. Rubinstein, J. L., Dickson, V. K., Runswick, M. J., and Walker, J. E. (2005) ATP synthase from *Saccharomyces cerevisiae*: Location of subunit h in the peripheral stalk region. *J. Mol. Biol. 345*, 513–520.
24. Velours, J., Vaillier, J., Paumard, P., Soubannier, V., Lai-Zhang, J., and Mueller, D. M. (2001) Bovine coupling factor 6, with just 14.5% shared identity, replaces subunit h in the yeast ATP synthase. *J. Biol. Chem. 276*, 8602–8607.
25. Cronan, J. E. (1990) Biotination of proteins in vivo. A post-translational modification to label, purify, and study proteins. *J. Biol. Chem. 265*, 10327–10333.
26. Adams, A., Gottschling, D., Kaiser, C., and Stearns, T. (1997) *Methods in Yeast Genetics*, pp 99−102, Cold Spring Harbor Laboratory Press, Plainview, NY.
27. Rubinstein, J. L. (2007) Structural analysis of membrane protein complexes by single particle electron microscopy. *Methods 41*, 409–416.
28. Crowther, R. A., Henderson, R., and Smith, J. M. (1996) MRC image processing programs. *J. Struct. Biol. 116*, 9–16.
29. van Heel, M., Harauz, G., Orlova, E. V., Schmidt, R., and Schatz, M. (1996) A new generation of the IMAGIC image processing system. *J. Struct. Biol. 116*, 17–24.
30. Frank, J., Radermacher, M., Penczek, P., Zhu, J., Li, Y., Ladjadj, M., and Leith, A. (1996) SPIDER and WEB: Processing and visualization of images in 3D electron microscopy and related fields. *J. Struct. Biol. 116*, 190–199.
31. Edgar, R. C. (2004) MUSCLE: Multiple sequence alignment with high accuracy and high throughput. *Nucleic Acids Res. 32*, 1792–1797.
32. Cuff, J. A., Clamp, M. E., Siddiqui, A. S., Finlay, M., and Barton, G. J. (1998) JPred: A consensus secondary structure prediction server. *Bioinformatics 14*, 892–893.
33. Straffon, A. F., Prescott, M., Nagley, P., and Devenish, R. J. (1998) The assembly of yeast mitochondrial ATP synthase: Subunit depletion in vivo suggests ordered assembly of the stalk subunits b, OSCP and d. *Biochim. Biophys. Acta 1371*, 157–162.

BI801665X